Phase-Matched Raman-Resonant Four-Wave Mixing in a Dispersion-Compensated High-Finesse Optical Cavity

Shin-ichi Zaitsu,[1] Hirotomo Izaki,[1] and Totaro Imasaka[1,2]

[1]*Graduate School of Engineering, Kyushu University, 744 Motooka, Nishi-ku, Fukuoka, Japan*
[2]*Center for Future Chemistry, Kyushu University, 744 Motooka, Nishi-ku, Fukuoka, Japan*

(Received 9 October 2007; published 19 February 2008)

A highly efficient intracavity four-wave mixing in a Raman-active medium pumped by a continuous-wave laser is first demonstrated. Managing the intracavity dispersion to satisfy the phase matching in a high-finesse cavity substantially enhances the anti-Stokes emission. This process is observed in a region far beyond small signal approximation, indicating the generation of phase-locked sidebands arising from molecular modulation. This points to a novel approach of an optical modulator and mode-locked laser operating at a frequency of more than 10 THz.

DOI: 10.1103/PhysRevLett.100.073901 PACS numbers: 42.65.Dr, 42.55.Ye

Four-wave mixing (FWM) has been attracting much attention as a typical $\chi^{(3)}$ nonlinear optical phenomenon since the advent of nonlinear optics. Several related phenomena, such as supercontinuum generation, optical phase conjugation, and coherent anti-Stokes Raman scattering (CARS), provide numerous useful approaches to control the nature of light in modern laser technology [1,2]. FWM originates from spatially or temporally modulated polarizability induced by incident multiple lightwaves; this property has practical spectroscopic [3] and microscopic [4] applications in studying a number of interactions of light with matter. To date, however, FWM has mainly been applied to such fruitful approaches using pulsed lasers with high instantaneous intensity because of the considerably low $\chi^{(3)}$ susceptibility of matter without resonance of electronic states. Since successful schemes [5–7] based on the continuous-wave (cw) laser have also been performed in the small signal region, where the intensity of anti-Stokes emission is infinitely lower than that of the pump emission, it has not been possible to strongly drive a FWM process using a cw laser as a pump source.

Frequency conversion of a cw laser by stimulated Raman scattering (SRS), which is also a $\chi^{(3)}$ nonlinear optical phenomenon, was achieved with a maximum efficiency of more than 60% using a double-resonance high-finesse optical cavity at a threshold below a mW level [8,9]. Since Raman-resonant FWM and SRS contribute equally to a Raman process [10], it is expected cw-based FWM will be achieved with a high efficiency using the same approach as that used in the cw-based SRS. In fact, Roos *et al.* suggested upconversion of a cw laser through an intracavity FWM process can be realized with an efficiency approaching the quantum limit (50%) [11]. Unfortunately, this theoretically predicted highly efficient cw-based FWM has not yet been achieved experimentally; this is because the efficiency of FWM in a high-finesse cavity is severely hindered by phase-mismatching among interactive fields (i.e., pump, Stokes, and anti-Stokes fields), arising from an inevitable frequency dependence of the refractive index of a Raman-active medium. Even for a gaseous medium that provides moderate chromatic dispersion, the coherence length of FWM interaction cannot exceed an effective pass length in a high-finesse cavity. Therefore, even when both pump and Stokes fields are sufficiently built up in the cavity, the growth of anti-Stokes emission through the FWM process is substantially limited.

In this Letter, we first demonstrate highly efficient FWM pumped by a cw laser using a dispersion-managed high-finesse cavity to achieve phase-matched interaction. The output power of cw anti-Stokes emission is more than a thousand times larger than the previously reported one [12]. It is also shown that the intracavity FWM process is observed in a region beyond small signal approximation. Although the result is essentially based on well-established CARS process, this highly efficient cw-based FWM process will open the possibility not only of up-conversion of a cw laser, but also of a high-speed optical modulator and high-repetition mode-locked laser operating at a frequency of more than 10 THz.

In the steady state limit, simple expressions can be obtained for intracavity powers of the pump and anti-Stokes fields by solving equations describing the coupling among monochromatic fields interacting with each other through Raman-active medium inside a dispersion-free optical cavity [11],

$$|E_p|^2 = \left(\frac{1}{1-x}\right)\frac{L_S}{G_1}, \tag{1}$$

$$|E_{AS}|^2 = x\frac{L_S}{L_{AS}}|E_S|^2, \tag{2}$$

where E_p, E_S, and E_{AS} are complex amplitudes of the pump, Stokes and anti-Stokes fields inside the cavity, respectively. L_S and L_{AS} ($L_S > L_{AS}$) are power losses due to one of cavity mirrors for the Stokes and anti-

Stokes emissions, respectively. G_1 represents Raman gain for the rotational Raman transition involving the pump and Stokes fields. x is an effective gain parameter which is defined by $x = L_S G_2 / L_{AS} G_1$, where G_2 is Raman gain for the transition involving the anti-Stokes and pump fields. Here parameter associated with phase matching in the FWM process for a single-pass length of the cavity is assumed to be unity. This assumption is valid in our case where the rotational Raman transition is considered with a relatively small Raman shift frequency (587 cm^{-1}) and a gaseous Raman-active medium is used providing negligible dispersion for a single-pass FWM interaction. These equations clearly imply that the efficient generation of anti-Stokes emission through an intracavity FWM process can be achieved if the dispersion effect of medium inside the cavity is ignored.

The free spectral range of a cavity is expressed as: $\mathrm{FSR}(\lambda) = c/2n_g(\lambda)l$, where c is the speed of light, $n_g(\lambda)$ is the group refractive index of a medium inside the cavity as a function of the wavelength, and l is the length of the cavity. This formula suggests longitudinal modes of the cavity containing a dispersive medium are not spaced at equal intervals. In contrast, in a Raman-resonant FWM process, it is necessary that frequencies of related fields, pump (ω_p), Stokes (ω_S) and anti-Stokes (ω_{AS}) fields are spaced at equal intervals: $\omega_{AS} - \omega_p = \omega_p - \omega_S$, owing to the phase-matching nature of a parametric interaction. This essential discrepancy does not allow all the fields related to the intracavity FWM process to match the cavity longitudinal modes [see Fig. 1(b)]. For instance, under a condition of 1 MPa of hydrogen gas, used as Raman-active medium, in an 8-cm cavity at a pump wavelength of 770 nm, the frequency difference between the anti-Stokes emission and closest longitudinal mode ($\Delta\Omega$) is estimated to be approximately 75 MHz. This is far beyond the linewidth (~100 kHz) of a high-finesse cavity required for cw Raman lasing. This mismatch essentially limits the output power of the anti-Stokes emission generated through a FWM process in a dispersive cavity. It should be noted here that, in the time domain picture, this explanation is equivalent to fact that the phase-matching condition is not satisfied over the full interaction length of the FWM interaction in a high-finesse cavity.

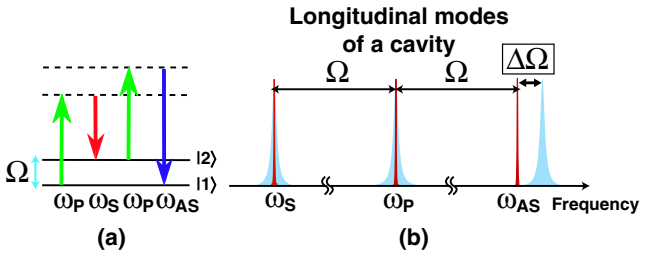

FIG. 1 (color online). (a) Energy diagram of Raman-resonant FWM. Ω: Raman shift frequency. (b) Simplified illustration of a relation between longitudinal modes of a high-finesse cavity and intracavity fields related to the FWM interaction.

One possible solution for this phase-mismatching problem is to use a dispersion-managed high-finesse cavity for the cw Raman lasing and intracavity FWM. In principle, perfect compensation to all orders of the total intracavity dispersion enables the longitudinal modes of the cavity to space at even intervals over the whole spectral range. Considering only the three fields (ω_S, ω_p, and ω_{AS}), however, a condition can be found in which the longitudinal modes related to these fields are equally separated by controlling only the second order of the intracavity dispersion (group delay dispersion, or GDD). Therefore, to achieve $\Delta\Omega = 0$, i.e., the efficient generation of the anti-Stokes emission, it is reasonable to use available chirped mirrors (CMs) with a negative GDD to compensate the positive GDD of a medium inside the cavity. In the experiment, a Fabry-Perot cavity ($l = 8$ cm) was used consisting of a pair of CMs (radius of curvature: 250 mm) designed to have a reflectivity of more than 0.9999 and a negative GDD of -20 ± 5 fs^2 in the near-infrared region (760–830 nm). This cavity was installed in a chamber with input and output silica windows. The chamber was filled with hydrogen gas, acting as a Raman-active medium, at a pressure of less than 1 MPa. A single-frequency Ti:sapphire laser (λ: 770 nm, linewidth <100 kHz) was used as a pump source. The beam (~200 mW) was coupled into the cavity using mode-matching optics after passing through a polarizer to ensure it to be linearly polarized. The GDD of hydrogen gas in the 8-cm length cavity at the wavelength of the Stokes emission (807 nm) is estimated to be ~10 fs^2 at a pressure of 1 MPa. Since this value was less than that of the CM used here, a slight amount of xenon gas was added to supply an additional GDD to the intracavity medium. A piezotransducer equipped to one of the CMs was driven to scan the cavity length so that the pump and Stokes emissions oscillated simultaneously. The partial pressure of hydrogen gas was then adjusted so that the total GDD in the cavity was zero.

According to Eq. (2), the ratio of the output power of the anti-Stokes emission (P_{AS}) to that of the Stokes emission (P_S) is a constant value determined by the losses of the cavity; i.e., it does not depend on the intracavity power of the pump field. In addition, $\Delta\Omega$ and total intracavity GDD can be approximated by a linear function of pressure of medium in the chamber including the cavity. Therefore, the etalon effect of the cavity on the total GDD can be observed by measuring P_{AS}/P_S while changing the pressure of the gaseous medium [see also Fig. 1(b)]. The measured power ratios (P_{AS}/P_S) were plotted as a function of the partial pressure of hydrogen gas in Fig. 2. The ratio was remarkably enhanced within the pressure range of a few tens of kPa in the vicinity of the optimized pressure. This plot is well consistent with the Airy function, describing the shape of a longitudinal mode of a cavity, with a full-width at half maximum ($\Delta\nu$) of 400 kHz. The $\Delta\nu$ agrees with the linewidth of a longitudinal mode of a cavity consisting of mirrors with a reflectivity of 0.9993, which

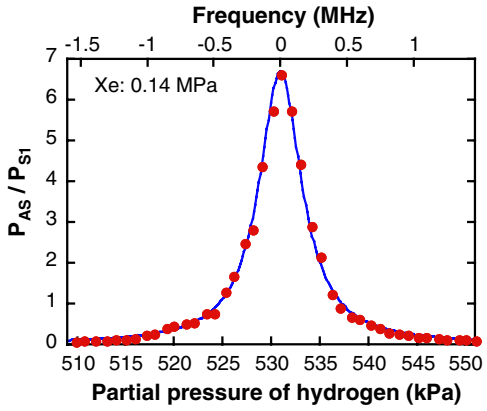

FIG. 2 (color online). The power ratio of the anti-Stokes and Stokes emissions (P_{AS}/P_S) as a function of the partial pressure of hydrogen (the lower abscissa axis). The corresponding frequency shift of $\Delta\Omega$ is shown in the upper abscissa axis. The partial pressure of xenon gas was 0.14 MPa.

corresponds to a designed value of the mirrors at the wavelength of the anti-Stokes emission. This clearly indicates the significant enhancement of the anti-Stokes emission is caused by matching the frequency of the anti-Stokes emission to one of the longitudinal modes of the cavity. The enhancement is also attributed to the equally spaced rearrangement of the related longitudinal modes arising from the dispersion management. Moreover, in the time domain picture, the result suggests the interaction distance of phase-matched FWM in the high-finesse cavity is substantially improved by the compensation of the dispersion of the Raman-active medium inside the cavity.

In this experiment, such a phase-matched intracavity FWM process was achieved under two different pressures of the medium inside the cavity. The output spectra measured under these conditions are shown in Figs. 3. The partial pressures of the hydrogen and xenon were 0.86 MPa and 0.1 MPa for Fig. 3(a), and 0.46 and 0.15 MPa for Fig. 3(b), respectively. As shown in the inset of Fig. 3(b), the anti-Stokes emission oscillated in a single transverse TEM_{00} mode that is the same as that of the pump and

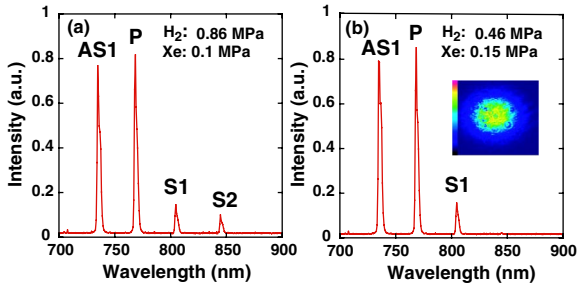

FIG. 3 (color online). The measured spectra of the output beams under different pressures of the intracavity medium. AS1: first anti-Stokes emission, *P*: pump emission, S1: first Stokes emission, and S2: second Stokes emission. The inset in (b) shows a beam profile of the anti-Stokes emission.

Stokes emissions. This indicates that high-order transverse modes did not contribute to the oscillation of the anti-Stokes emission. When the cavity length is 8 cm, the GDD is 10 fs^2 for hydrogen and 80 fs^2 for xenon at a pressure of 1 MPa; these GDDs have a nearly linear dependence on their pressures, at least for less than 1 MPa. Since the total GDD in the cavity can be approximated by the sum of each GDD, it is estimated to be 16.6 fs^2 for both cases. This value corresponds to the designed value of a negative GDD of the CMs used here. Therefore, it is determined that the efficient generation of the anti-Stokes emission is due to the compensation of the intracavity GDD.

Figure 4 shows the evolution of the output power of each emission as a function of the total output power, which was measured while changing the resonant condition by scanning the length of the cavity. The figure shows the dependence is divided into three regions. Although the first region below the threshold of the first Stokes emission is trivial, the behaviors of each emission in the second and third regions specifically show how the intracavity FWM is different from conventional FWM. In the second region between the thresholds of the first and second Stokes emissions, the constant power of the pump emission (P_p) agreed with the prediction from Eq. (1) in that the intracavity power of the pump field was clamped above the threshold. In addition, both P_S and P_{AS} increased linearly, which agrees also with Eq. (2), suggesting $|E_{AS}|^2/|E_S|^2$ was constant. Here, using $R_{AS} = 0.9993$ from the result described in the previous paragraph and $R_S = 0.999\,915$ from the measured linewidth of the cavity at the wavelength of the Stokes emission, L_S/L_{AS} is estimated to be $\sim$0.13. This gives, from Eq. (2), the ratio of the intracavity power of the anti-Stokes emission to that of the Stokes emission ($|E_{AS}|^2/|E_S|^2$) as approximately 1.7×10^{-2} under the assumption of $G_1 \simeq G_2$ and the phase-matching condition. On the other hand, the measured power ratio

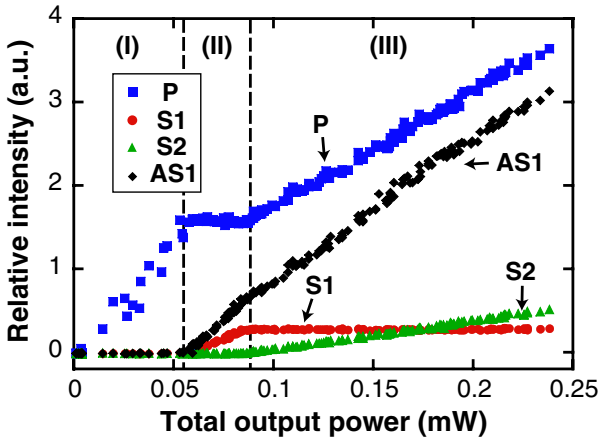

FIG. 4 (color online). Intensities of each emission as a function of the total output power. *P*: pump laser, S1: first Stokes emission, S2: second Stokes emission, and AS1: first anti-Stokes emission.

outside the cavity was ~2.5. Since the output power ratio is obtained by multiplying the ratio of transmittances for each emission to the intracavity power ratio, the scattering and absorption loss at the mirror is calculated as ~80 ppm.

In the third region above the threshold of the second Stokes emission, P_S was clamped and P_p increased linearly with an increase in the power of the second Stokes emission. P_{AS} also increased with a slope slightly different from that in the second region. To explain this dependence of P_{AS} on the intracavity power of the pump field in this region, the following equation can be used, obtained by combining Eqs. (1) and (2),

$$|E_{AS}|^2 = G_1 G_2 \left(\frac{|E_p|^2}{L_{AS} + G_2 |E_p|^2} \right)^2 |E_S|^2. \quad (3)$$

According to this equation, since $|E_S|^2$, G_1, G_2 and L_{AS} is constant, $|E_{AS}|^2$ is determined by a variable parameter $|E_p|^2$. If $L_{AS} \gg G_2 |E_p|^2$, Eq. (3) is approximated to $P_{AS} \propto P_p^2 P_S$ that is generally used to describe the behavior of the anti-Stokes emission in the small signal region [3]. In our experiment, however, the evolution of P_{AS} showed no quadratic dependence on the intracavity pump power, indicating L_{AS} and $G_2 |E_p|^2$ had comparable contributions to the generation of the anti-Stokes emission. This also suggests the energy transfer from the anti-Stokes emission to the pump emission through a SRS process was not negligible in this intracavity Raman-resonant FWM process. It clearly proves that the intracavity FWM process demonstrated here has a remarkably high efficiency far beyond the small signal region, which is the first demonstration in a FWM process pumped by a cw laser.

At this time, the maximum output power of the anti-Stokes emission is limited to ~100 μW. This was mainly due to the significant loss (~80 ppm) of the CMs used in the experiment. Reduction of this undesirable loss of the mirror and optimization of the input power will enable an up-conversion efficiency approaching 50% to be obtained, which was theoretically predicted in the previous literature [11]. Such a highly efficient conversion is quite useful for a light source emitting at a wavelength that is difficult to obtain by conventional semiconductor lasers. Another promising application of phase-matched intracavity FWM is emphasized here, that being an optic-modulator operating at a frequency in a terahertz region. The phase relation between a pump field and Raman sidebands is essentially locked because of the nature of a parametric interaction in the Raman-resonant FWM process that requires phase matching among related fields. Accordingly, the generation of our multifrequency cw emissions can be interpreted as a result of the lightwave modulation induced by a time-dependent refractive index based on coherent molecular motions. This indicates a highly efficient intracavity FWM process allows the modulation of a cw lightwave at a frequency of molecular motion that generally ranges over 10 THz [13]. From the same point of view, this modulation mechanism can also be used for synthesizing a pulse train with a repetition rate of more than 10 THz [14]. We conceive that the output beam obtained in this experiment surely forms an ultrashort pulse train with a duration of ~30 fs at the repetition rate corresponding to the rotational frequency of hydrogen, 17.6 THz, in a cw mode. We have already observed the generation of five frequency components in the previous experiment, although the output powers of some components were extremely low [15]. This implies the broadening of the bandwidth of a dispersion-compensated high-finesse cavity will allow us to generate phase-locked multifrequency emissions. This approach opens a possibility of producing an extremely high-repetition mode-locked laser including a novel modulation mechanism using coherent molecular motions.

In conclusion, a cw Raman-resonant FWM process was first observed in an optical cavity for which the dispersion was managed. The anti-Stokes emission through an intracavity FWM process was remarkably enhanced in the dispersion-compensated cavity filled with a gaseous Raman-active medium. It was also pointed out that the intracavity fields interacted in a region far beyond the small signal approximation, which has never been achieved in a conventional cw-based FWM process. This process will be sufficiently efficient to provide new promising applications, e.g., upconversion to inaccessible wavelengths, ultra high-speed modulation of lightwaves, and generation of a pulse train at an extremely high repetition rate.

This research was supported by Grants-in-Aid for Scientific Research and the 21st Century COE Program from the Ministry of Education, Culture, Science, Sports and Technology of Japan.

[1] Y. R. Shen, *The Principle of Nonlinear Optics* (Wiley-Interscience, New Jersey, 2003).
[2] R. W. Boyd, *Nonlinear Optics* (Academic, San Diego, 2003).
[3] W. M. Tolles *et al.*, Appl. Spectrosc. **31**, 253 (1977).
[4] J. X. Cheng and X. S. Xie, J. Phys. Chem. B **108**, 827 (2004).
[5] R. Claps *et al.*, Opt. Express **11**, 2862 (2003).
[6] J. J. Barrett and R. F. Begley, Appl. Phys. Lett. **27**, 129 (1975).
[7] T. S. Bican *et al.*, J. Raman Spectrosc. **26**, 699 (1995).
[8] J. K. Brasseur *et al.*, Opt. Lett. **23**, 367 (1998).
[9] L. S. Meng *et al.*, Opt. Lett. **26**, 426 (2001).
[10] N. Bloembergen and Y. R. Shen, Phys. Rev. Lett. **12**, 504 (1964).
[11] P. A. Roos *et al.*, J. Opt. Soc. Am. B **21**, 357 (2004).
[12] J. K. Brasseur *et al.*, J. Opt. Soc. Am. B **17**, 1223 (2000).
[13] D. D. Yavuz, Phys. Rev. A **76**, 011805(R) (2007).
[14] K. Shinzen *et al.*, Phys. Rev. Lett. **87**, 223901 (2001).
[15] S. Zaitsu *et al.*, J. Opt. Soc. Am. B **24**, 1037 (2007).